

# Design and Fabrication of Stent with Negative Poisson's Ratio

S. K. Bhullar, J. Ko, F. Ahmed, M. B. G. Jun

**Abstract**—The negative Poisson's ratios can be described in terms of models based on the geometry of the system and the way this geometry changes due to applied loads. As the Poisson's ratio does not depend on scale hence deformation can take place at the nano to macro level the only requirement is the right combination of the geometry. Our thrust in this paper is to combine our knowledge of tailored enhanced mechanical properties of the materials having negative Poisson's ratio with the micromachining and electrospinning technology to develop a novel stent carrying a drug delivery system. Therefore, the objective of this paper includes (i) fabrication of a micromachined metal sheet tailored with structure having negative Poisson's ratio through rotating solid squares geometry using femtosecond laser ablation; (ii) rolling fabricated structure and welding to make a tubular structure (iii) wrapping it with nanofibers of biocompatible polymer PCL (polycaprolactone) for drug delivery (iv) analysis of the functional and mechanical performance of fabricated structure analytically and experimentally. Further, as the applications concerned, tubular structures have potential in biomedical for example hollow tubes called stents are placed inside to provide mechanical support to a damaged artery or diseased region and to open a blocked esophagus thus allowing feeding capacity and improving quality of life.

**Keywords**—Micromachining, electrospinning, auxetic materials, enhanced mechanical properties.

## I. INTRODUCTION

### A. Problem Area

**S**TENTS are usually defined as small tubular structures that are inserted into the diseased region which provide mechanical support to damaged artery or for the palliation of dysphagia from inoperable esophageal or gastric cardiac cancer. The use of stents for esophageal diseases has evolved greatly over the past 30 years. For a brief description esophagus is the tube that runs from the mouth to the stomach and it carries food we swallow to our stomach to be digested. Esophageal cancer is the growth of cancer cells in esophagus tube which usually originates in the inner layers of the lining of the esophagus and grows outward. In time, the tumor can obstruct the passage of food and liquid, making swallowing painful and difficult. About 13,000 new cases of esophageal cancer are diagnosed in the United States each year [1]. Since most patients are not diagnosed until the late stages of the disease, esophageal cancer is associated with poor quality of

life and low survival rates. Treatment, therefore, focuses mainly on palliation therapy of dysphagia employing a stent to mechanically open a blocked esophagus as illustrated in Fig. 1, thereby allowing feeding capacity and improving quality of life. Studies are being performed to improve stent patency and to mitigate stent related complications. A number of studies have employed to study the influence of stent design parameters on the mechanical performance of a stent. To mention a few – the effect of stent design parameters on arterial wall stress and radial displacement of the stent was discussed in [2], [3]. The role of the three-dimensional draping (prolapse) of the stented artery has been analyzed in [4] through finite element analysis. Comparison of stent parameters with stresses imposed on the arterial wall [5], multi-Link stent had lower stresses and a lower rate of restenosis [6] and longitudinal strain in stents during deployment via balloon catheter has been studied in [7]. Also, a stent with a negative Poisson's ratio for more precise deployment using finite element analysis [8], [9] and a model of an auxetic stent of rotating-square geometry with a circular hole of polyurethane are discussed in [10]. Further, various types of esophageal stents made of metal, plastic or bioabsorbable polymer, have been technically evolved and many of them are already in clinical use to relieve dysphasia [11]. These stents are designed to possess good mechanical flexibility for ease of insertion and elimination of excessive esophagus dilation. Also, metal stents have become popular for the palliation of patients with malignant esophageal obstruction, especially patients with a poor prognosis [12]. Insertion of a self-expandable metal stent (SEMS) has become a well-established technique over the past 10 years. The major advantage of stent insertion is that it offers rapid improvement in dysphagia, and SEMS have a relatively low procedure-related complication rate [13]. Early, delayed and Potentially life-threatening complications associated with stent placement are misplacement, perforation, chest pain, stent migration, occlusion of the stent due to tumor in-growth and out-growth or food impaction [14]-[16]. Therefore, it is a major current challenge to develop, design and manufacture such stents that are maximally compatible with living tissue, light weight, reduce migration and get a good grip with tumor tissue. Studies and experiences demonstrated smart materials with a negative Poisson's ratio called auxetic materials which become wider when stretched along with enhanced mechanical properties such as synclastic behavior, resilient nature and stiffness without brittleness are good candidate for biomedical industry [17], [18].

S. K. Bhullar is with Department of Mechanical Engineering, University of Victoria, V8W 3P6, Victoria, BC, Canada and with the Department of Mechanical Engineering, Bursa Technical University, Bursa, Turkey (Corresponding author e-mail: sbhullar@uvic.ca).

J.Ko, F. Ahmed Bhullar, and M.B.G. Jun Bhullar are with Department of Mechanical Engineering, University of Victoria, V8W 3P6, Victoria, BC, Canada.

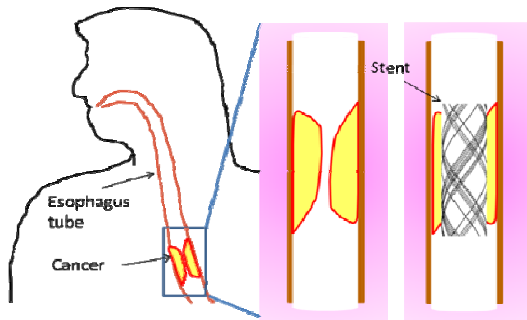


Fig. 1 A tube (stent) can be used to hold open a narrowed portion of the esophagus

### B. Auxetic Materials and Structures

Auxetic materials with tailored negative Poisson's ratio offer a huge potential in biomedical in designing of stents, scaffolds and implants. This unusual, behavior has been an accepted consequence of classical elasticity theory for over 150 years [19] and they are thermodynamically stable materials. In fact Poisson's ratios of isotropic materials can not only take negative values, but can have a range of negative valuestwice that of positive ones [20]. To date a variety of auxetic materials and structures have been discovered, fabricated or synthesized ranging from the microscopic down to the molecular levels. All major classes of materials (polymers, composites, metals, and ceramics) can exist in auxetic form [17], [21]. However, natural auxetic materials do exist, for example the single crystals of arsenic, cadmium and alpha-cristobalite [22]-[24] as well as some very important biological materials such as skin- cat skin, cow teat skin, salamander skin and load-bearing cancellous bone from human shins [25]-[28]. Another example is the arterial endothelium when subjected to both wall shear stresses and a cyclic circumferential strain due to pulsatile blood flow [29]. In the biomedical field auxetic micro-porous and cellular materials have potential, such as a dilator for opening the cavity of an artery or similar vessels, scaffolds, implants and stents. To exemplify an auxetic scaffold or stent would expand and contract in tandem with the strains resulting from the cyclical pressures from pulsatile blood flow. Thus, an auxetic scaffold that exhibits concurrent axial and transverse expansion (contraction) would likely better integrate with native tissues and better promote clinical tissue regeneration. Other examples where auxetic constructs could be useful are in myocardial (as an auxetic cardiac patch), skin and fat tissue engineering and in wound management [30]-[33] as well. However, limited work has been performed to design, fabricate, and study auxetic metal structures in smart stent applications.

In this paper, design and fabrication of a metal stent with negative Poisson's ratio is achieved by designing an auxetic structure with rotating squares geometry theoretically developed in [34]. Fabrication of a stent by welding auxetic metal structure into a tubular shape and then loaded with nanofibers for drug delivery is then presented, followed by performance analysis of the fabricated stents. Then, the results

are discussed followed by some conclusions. To our knowledge combination of Femtosecond laser machining ablation technique for creating auxetic (rotating-squares) geometry in fabrication of auxetic stent and solution electrospinning process to wrap the fabricated stent with nanofibers of polymers for drug delivery have never been reported.

## II. METHODOLOGY

### A. Design of the Auxetic Structure

In order to implement auxetic property, structural design is tailored through angled solid squares. The auxetic behavior is based on an arrangement involving repeating squares connected together at their vertices by hinges. Each unit cell contains four squares, each square contains four vertices, and two vertices correspond to one hinge, as illustrated in Fig. 2 is designed using the SolidWorks engineering software. On application of uniaxial loads, these 'rigid squares' rotate with respect to each other to form a more open structure hence giving rise to a negative Poisson's ratio.

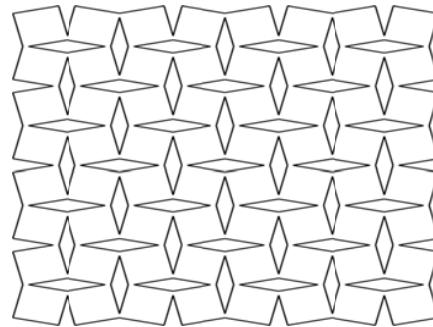


Fig. 2 Arrangement involving repeating squares connected together at their vertices by hinges

### B. Fabrication of Auxetic Sheet

The auxetic structures were fabricated on a flat sheet of stainless steel 316, which is a biocompatible material used in many biomedical applications. The sheets ( $64\text{mm} \times 45\text{mm} \times 0.127\text{mm}$ ) and ( $25\text{mm} \times 18\text{mm} \times 0.127\text{mm}$ ) having unit cell of four squares hinged at their corners having angle between two such squares  $\theta = 28^\circ$  and aligned in the plane as illustrated in Fig. 3, were used to prepare samples using femtosecond laser machining. Femtosecond pulse laser ablation can yield precise materials processing resulting from efficient energy deposition, while simultaneously minimizing heat conduction and thermal damage to the surrounding material. The femtosecond laser (Spectra-Physics ultrafast Ti: Sapphire laser) system is shown in Fig. 4. The kilohertz ultrafast laser has a pulse width of 120 femtosecond with a center wavelength of 800nm. A set of neutral density (ND) filters was used to tune the output laser power to a value suitable for stent manufacture. A computer controlled electronic shutter was used to selectively turn on/off the laser beam. An iris diaphragm was used to reduce beam diameter to 6mm. Then the laser beam was guided into and focused by a

microscope objective lens (numerical aperture: 0.42). The sample was mounted on a computer controlled 3-axis stage and the software, LaserCAM was used to generate scanning path of the laser head. The stent fabrication was done with an average laser power of 0.5 watts and scanning speed of 200 $\mu$ m/sec using 6 passes, each vertically offset by 20 $\mu$ m. The features fabricated during focused irradiation of femtosecond pulses were monitored using a CCD camera mounted above the dichroic mirror. The fabricated samples then cleaned with acetone in an ultrasonic bath and analyzed using an optical microscope. Pictures of 'rotating rigid squares' using optical microscope and their microscopic images are shown in Fig. 5.

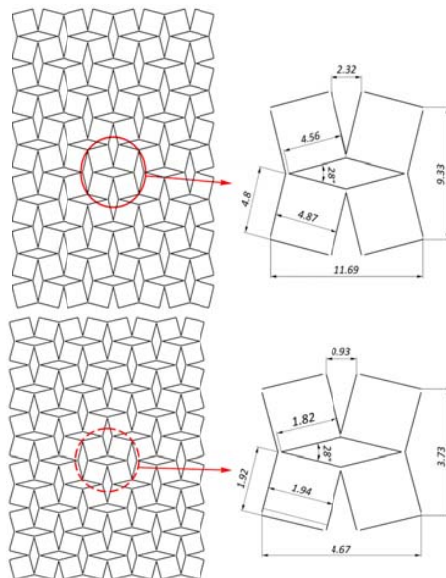


Fig. 3 Samples of auxetic structures of rotating squares and a unit cell of the structure

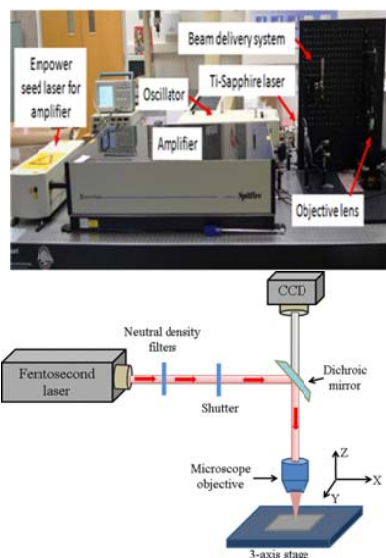


Fig. 4 The femtosecond laser system and laser machining set up

### C. Fabrication of Auxetic Cylindrical Stent

Next, prepared auxetic metal structure was rolled and welded using laser welding to a stent form as shown in Fig. 6. Annealing to ease or remove the stresses on the auxetic stent due to the welding has been taken in consideration. Pictures of fabricated auxetic stent using optical microscope are shown in Fig. 6 as well.

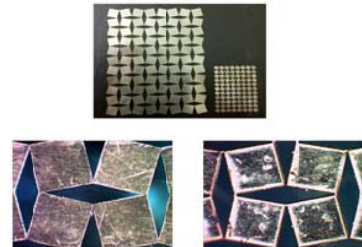


Fig. 5 Fabricated auxetic rotating rigid squares structures

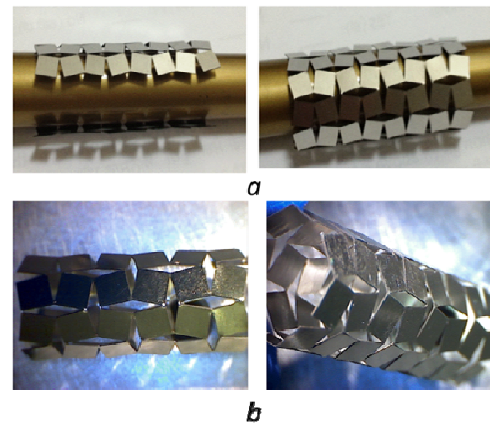


Fig. 6 Wooden rod wrapped with Auxetic sheet and Auxetic stent after welding (top); Microscopic pictures of auxetic rotating rigid squares structures (bottom)

### D. Wrapping of Tents with Nanofibers

Further, for almost all cases, the esophageal stents suffer from reocclusion due to rapid growth of tumors around the stent to shorten the effective lifespan of the treatment, hence multiple of major surgeries for stent replacement [15]. In this sense, local and sustained delivery of an anti-cancer agent would be advantageous to suppress the tumor growth around the esophageal stent. In such systems, the drug would be released specifically towards the cancerous tissues in the esophagus, possibly achieving effective drug bioavailability around a stent for a prolonged period of time without unnecessarily high systemic drug exposure. Porous and flexible coating or mesh on the stent can be used for such purposes. Therefore, the fabricated auxetic stent was wrapped with nano-fibers of biocompatible polymer using solution electro- spinning. The electrospinning system is shown in Fig. 7. PCL,  $M_n = 45000$  was purchased from Aldrich Chemical Co, USA; Chloroform from Fisher Scientific, Canada; Methanol from VWR International, Canada. A mixture solvent

of Chloroform and Methanol with a volume ration of 7:1 was prepared to dissolve 10 % PCL (w/v) in the mixed solvent. PCL solution was stirred overnight at room temperature at 1100 rpm.

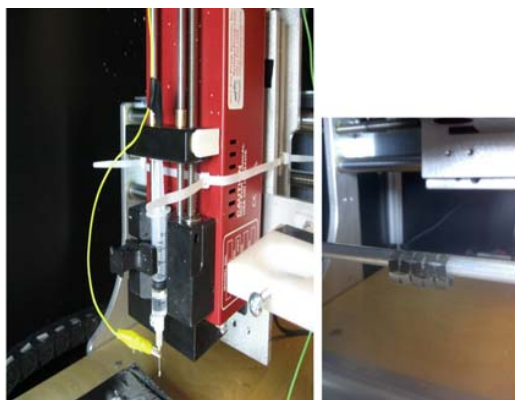


Fig. 7 Electrospinning system and set up of stent sample

The experimental setup, operated to fabricate the electrospun PCL nanofibers, is schematically described in Fig. 8. The setup consists of a syringe pump (New Era Pump Systems Inc., USA), stainless steel needles (McMaster-CARR, Canada), drum fiber-collector machined aluminum with DC motor for wrapping of stent with nanofibers, and a high voltage power supply (GAMMA High Voltage Research Inc., USA). The stainless steel needle receives the polymer solution through a syringe connected to the syringe pump, which maintains the constant flow rate of the polymer solution to the tip of needle. In order to wrap stent with nanofibers, the machined stent is mounted on drum fiber-collector which is placed below needle tip. The distance between them is fixed at optimizing conditions based on our preliminary results. The positive terminal of the high voltage power supply (0-30kV) is connected to the drum while the ground terminal is connected to the needle tip.

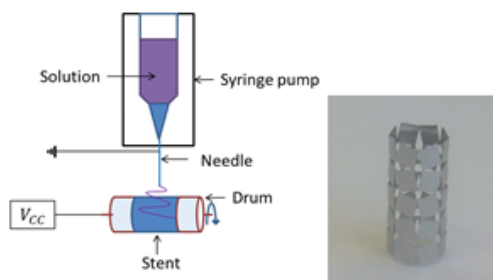


Fig. 8 Schematic representation of the device used for the electrospinning of PCL nanofibers on a stent and stent wrapped with nanofibers

#### E. Tensile Testing

For further analysis, conventional macro-tensile measurements were performed using an electromechanical tensile tester (Adelaide Testing Machines, Toronto, Ontario, Canada). All samples were mounted between holders at a

distance of 3cm. Tensile testing was conducted at a rate of 2mm/min at room temperature (21°C) and at two times each. The amounts of elastic modulus and strain at the breaking point were calculated by the Adelaide Testing Machines software. The Yield strength test for both sample 1 and sample 2 was performed and stress and strain curves from collected data are shown in Figs. 9 and 10. Each elastic modulus for sample 1 and 2 are 3.5Mpa/mm and 20.8Mpa/mm. The sample 1 and 2 are respectively stretched until 5.8mm and 3.2mm by changing the shape of structure at 3.8MPa and 10.1MPa as elasticity section. After elasticity section, the sample 1 and 2 are completely deformed as shown in Figs. 9 (C) and 10 (C).

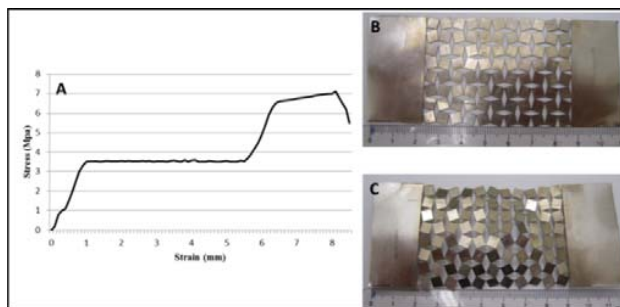


Fig. 9 Results of Sample 1 without endtabs(64mm × 45mm × 0.127mm), (A) Stress-strain curve, (B) Original sample, (C) Stretched sample

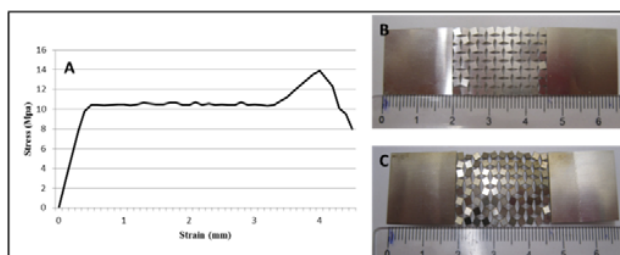


Fig. 10 Results of Sample 2 without endtabs(25mm × 18mm × 0.127mm), (A) Stress-strain curve, (B) Original sample, (C) Stretched sample.

#### F. Analytical Solution

The mechanism for producing a negative Poisson's ratio is not scale-dependent, so it exhibiting exactly the same geometry and deformation mechanism at the macro-, micro- and nano- (molecular) level. Further, for simple structures deformation mechanisms the magnitude of the Poisson's ratio can be easily identified from a visual analysis the structure and material. However, when the geometry of the structures is more complex than magnitude of Poisson's ratio can be obtained by deriving analytical equations in terms of the structure's geometrical parameters. The shape of the structure for various values of  $\theta$  (as shown above in Fig. 3) may be obtained through loading in a direction and the projections of the unit cell in the  $X_i$  directions are given in [35], [36]:

$$X_1 = X_2 = 2a \left[ \cos\left(\frac{\theta}{2}\right) + \sin\left(\frac{\theta}{2}\right) \right] \quad (1)$$



and structure that deforms solely by relative rotation of the squares, then  $a$  is constant and hence  $X_1$  are functions of the single variable  $\theta$ . Also, the stiffness of the structure (and hence the Young's moduli) may be related to the stiffness of the hinges, that is, a stiffness which opposes changes in the angles  $\theta$  and hinges satisfy the equation:

$$M = K_h(\delta\theta) \quad (2)$$

where,  $M$  is the moment applied to the rectangles,  $\delta\theta$  is the angular displacement due to  $M$ , and  $K_h$  is the spring constant for the hinge. As the structure only deforms through relative rotation of the rigid squares, the structure is geometrically not allowed to shear. This results in an infinite on-axis shear modulus and a value of zero for the five elements of compliance matrix which are associated with shearing. The compliance matrix for this system is hence of the form:

$$S = [S_{ij}] = \begin{bmatrix} \frac{1}{E_1} & -\frac{\nu_{21}}{E_1} & 0 \\ -\frac{\nu_{12}}{E_1} & \frac{1}{E_2} & 0 \\ 0 & 0 & 0 \end{bmatrix} \quad (3)$$

where,  $\nu_{ij}$  and  $E_i$  represents the Poisson's ratios and Young's modulus in the  $Ox_{ij}$  plane for loading in the  $Ox_i$  direction.

The infinitesimally small strains  $d\varepsilon_i$  in the  $Ox_i$  directions is defined by:

$$d\varepsilon_i = \frac{dX_i}{X_i} \text{ and } X_i = X_i(\theta) \quad (4)$$

Therefore, Poisson's ratio is obtained as:

$$\nu_{21} = \nu_{12} = -\frac{dX_1/X_1}{dX_2/X_2} \quad (5)$$

Further, the work done by each unit cell due to the changes in the inter-square angles from  $\theta$  to  $\theta + d\theta$  that accompany a small strain is given in [36]:

$$W = N \left[ \frac{1}{2} K_h (d\theta)^2 \right] \quad (6)$$

where,  $N$  is the number of hinges per unit cell. The principle of conservation of energy is

$$U = \frac{1}{V} W \quad (7)$$

where,  $V$  is the volume of the unit cell. Also for loading in the  $Ox_i$  direction work done per unit volume due to infinitesimal small strain is given by

$$U = \frac{1}{2} E_i \frac{1}{X_i} \left( \frac{dX_i}{d\theta} \right)^2 (d\theta)^2 \quad (8)$$

Hence the Young's modulus  $E_i$  ( $i = 1, 2$ ) from (6) to (8) are given by:

$$E_i = NK_h \frac{X_i^2}{X_1 X_2} \left( \frac{dX_i}{d\theta} \right)^{-2}, \quad i = 1, 2. \quad (9)$$

### III. RESULT AND DISCUSSION

The stenting outcomes were improved through mechanical design with tailored negative Poisson's ratio through cell geometry of the fabricated stent. The aim of this study was fourfold: (i) designing and manufacturing an micromachined auxetic structure; (ii) configuring this auxetic structure as an auxetic stent for the treatment of esophageal cancer and for the prevention of dysphagia and (iii) wrap auxetic stent with nano fibers for drug delivery to control further growth of tumor (iv) To compare the physical tests of the auxetic stent with analytical results of stent to achieve an agreement between the physical and analytic results. The metal structure is fabricated on a flat sheet of stainless steel 316, was selected as a material after doing a literature review which is a biocompatible material used in many. The values of Poisson's ratio and Young's modulus obtained through tensile testing are given in Table I for both samples. It is noticed that these values are close to the analytical values in the case of sample 2 which is one fourth of the size of the sample 1.

TABLE I  
VALUES OF POISSON'S RATIO

	Analytically		Experimentally	
	Poisson's ratio	Young's modulus	Poisson's ratio	Young's modulus
Sample 1	-1	4.1MPa/mm	-0.71	3.6MPa/mm
Sample 2	-1	16.7MPa/mm	-1.041	20.8MPa/mm

Since negative values of Poisson's ratio are achieved through the tailored auxetic geometrical structure, hence due to deformation mechanism the diamond shaped cuts within the geometry of the sample were wide opened which is visualized through microscopic images illustrated in Fig. 11.

In addition, the enhanced mechanical properties achieved through auxeticity such as the synclastic behavior of auxetic structure to be advantageous in terms expansion inside the esophageal lumen wall evenly from each side.

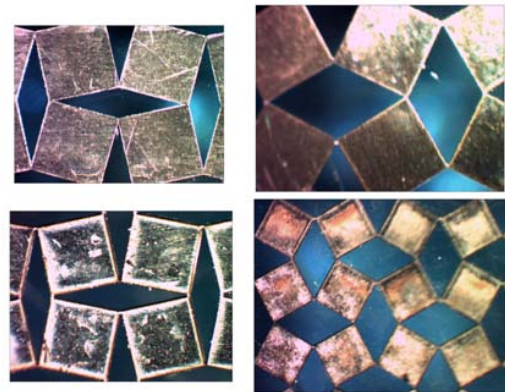


Fig. 11 Rotating hinging squares mechanism, sample 1 and sample 2

To summarize the results due to the unique deformation mechanism and the geometry of the auxetic stent would be:

- (i) The large (expandable) diameter could be obtained and it can be helpful to reduce complications like food impaction, and obstruction.
- (ii) Under uniaxial tensile loading, synclastic behaviour of auxetic stent would be advantageous in terms of auxetic stent expansion inside the esophageal lumen wall evenly from each side.
- (iii) On stretched longitudinally it will get bigger and wider, and get the anchorage with the surrounding tumor tissue inside the esophagus. It could be helpful to get a good grip with tumor tissue by embedding inside the tissue.
- (iv) On extending the drug loaded auxetic fibres will open the micropores and a specific dose of drug will be released specifically towards the cancerous tissues and on relaxing drug delivery will be ceased. Due to novel expansion behavior in both ways, transversely and longitudinally it will dilate the esophagus by itself. In addition, it can also work like a drug carrying system to dispense targeted local chemotherapy through its wrapped nano fibers directly from the stent surface to the neighboring malignant tissue instead of painful systemic chemotherapy procedure.

#### IV. CONCLUSION

This paper demonstrates successful design and fabrication of an auxetic stent with drug carrying system achieved through the combination of micromaching and electrospinning techniques. Its structure has specifically tailored mechanical properties which are achieved through auxeticity shows enhanced functional performance. In addition initially having a small diameter fabricated stent could be beneficial in deployment while its expandable diameter achieved through deformation mechanism could get good grip with tumor tissue; hence, it could improve quality of life.

#### ACKNOWLEDGEMENTS

The authors acknowledge financial support of Discovery and Engage programs of Natural Science and Engineering Research Council of Canada (NSERC).

#### REFERENCES

- [1] Müller J. M., Erasmi H., Stelzner M., Zieren U. and Pichlmaier H. 1990 Surgical Therapy of Oesophageal Carcinoma *Br. J. Surg* 77 845-57.
- [2] Sundelöf M, Ringby D, Stockled D, Gransröm, Jonas E and Freedom J 2007 Palliative Treatment of Malignant Dysphagia with Self-Expanding Metal Stents: A 12-Year Experience", *Scand J Gastroenterol*, 42 11-16.
- [3] Berry J L, Manoach E and Mekkaoui C 2002 Hemodynamics and Wall Mechanics of a Compliance Matching Stent: In Vitro and In Vivo Analysis", *J. Vasc. Interv. Radiol* 13 97-105.
- [4] Bedoya J, Meyer CA and Timmins LH 2006 Effects of Stent Design Parameters on Normal Artery Wall Mechanics. *J Biomech Eng*. 128 757-765.
- [5] Lally C, Dolan F and Prendergast P J 2005 Cardiovascular Stent Design and Vessel Stresses a Finite Element Analysis *J Biomech* 38 1574-1581.
- [6] Holzapfel GA, Stadler M. and Gasser TC 2005 Changes in the Mechanical Environment of Stenotic Arteries during Interaction with Stents: Computational Assessment of Parametric Stent Designs *Journal of Biomech Eng*. 127 166-180.
- [7] Migliaiaca F, Petrini L, Colombo M, Auricchio F and Pietrabissa R, 2002 Mechanical Behavior of Coronary Stents Investigated through the Finite Element Method *Journal of Biomechanics* 35 803-811.
- [8] Binzoni T, Leung T S, Boggett D and Delpy D T 2002 A New Near Infrared Laser-Doppler Flowmeter for Deep Tissue Perfusion Monitoring *MAGMA* 14 74-75
- [9] Murtaza NA and Ihtesham UR 2011 An Auxetic Structure Configured as Oesophageal Stent with Potential to Be Used for Palliative Treatment of Oesophageal Cancer; Development and *in vitro* Mechanical Analysis *J Mater Sci Mater Med* 22 2573-2581.
- [10] Raamachandran J and Jayavenkateshwaran K 2007 Modeling of Stents Exhibiting Negative Poisson's Ratio Effect *Computational Methods Biomechanics Biomed. Eng.*, 2007; 10: 245-255.
- [11] Bhullar SK, Mawanane AT Hewage, Alderson A, Alderson and Martin BG Jun, 2013, Influence of Negative Poisson's Ratio on Stent Applications *Advances in Materials*, doi: 10.11648/j.am.20130203.14 2(3) 42-47.
- [12] Conigliaro R, Battaglia G and Repici A 2007 Polyflex Stents for Malignant Oesophageal and Oesophagogastric Strictures: A Prospective, Multicentric Study *Eur J Gastroenterol Hepatol* 19 195-203.
- [13] Eberhart RC, Su SH, Nguyen KT, Zilberman M, Tang L, Nelson KD and Frenkel P 2003 Review-Bioresorbable Polymeric Stents: Current Status and Future Promise *Journal of Biomaterials Science, Polymer Edition* 14 299-312.
- [14] Kastrati A, Mehilli J, Dirschinger J, Pache J, Ulm K, Schühlen H, Seyfarth M, Schmitt C, Blasini R, Neumann FJ and Schömig A 2001 Restenosis After Coronary Placement of Various Stent Types," *American Journal of Cardiology* 87 34-39.
- [15] Pan Y, Dong S, Hao Y, Chu T, Li C, Zhang Z and Zhou Y 2010 Demineralized Bone Matrix Gelatin as Scaffold for Tissue Engineering *African Journal of Microbiology Research* 4 (9) 865-870.
- [16] Morgan R and Adam A 2001 Use of Metallic Stents and Balloons in the Esophagus and Gastrointestinal Tract *J Vasc Interv Radiol* 12 283-97.
- [17] Kostopoulos PP, Zissis MI, Polydorou AA, Premchand PP, Hendrickse MT, Shorrock CJ and Isaacs PE 2003 Are Metal Stents Effective for Palliation of Malignant Dysphagia and Fistulas? *Dig Liver Dis* 35(4) 275-82
- [18] Lakes R S 1987 Foam Structures with A negative Poisson's Ratio *Science* 235 1038-1040.
- [19] Lakes R S Design Considerations for Negative Poisson's Ratio Materials *ASME J. Mech. Design* 115 696-700.
- [20] Love A E H 1944 *A Treatise on the Mathematical Theory of Elasticity* (Dover: New York), p 163.
- [21] Fung Y C 1968 *Foundations of Solid Mechanics* (Prentice-Hall), p 353.
- [22] Caddock B D and Evans K E 1989 Microporous Materials with Negative Poisson's Ratios I: Microstructure and Mechanical Properties *J. Phys. D: Appl. Phys.* 22 1877-1882.
- [23] Gunton D J and Saunders G A 1972 The Young's Modulus and Poisson's Ratio of Arsenic, Antimony and Bismuth *J. Mater. Sci* 7 1061-1068.
- [24] Li Y, 1976 The Anisotropic Behavior of Poisson's Ratio, Young's Modulus, and Shear Modulus in Hexagonal Materials *Physica Status Solidi A* 38 171-175.
- [25] Yeganeh-Haeri Y, Weidner DJ and Parise JB 1992 Elasticity of Cristobalite Silicon Dioxide with a Negative Poisson's Ratio *Science* 257 650-652.
- [26] Veronda DR and Westmann RA 1970 Mechanical Characterization of Skin Finite Deformations *J. Biomech.* 3 111-124
- [27] Frohlich LM, Labarbera M and Stevens WP, 1994 Poisson's Ratio of a Crossed Fibre Sheath: The Skin of Aquatic Salamanders *J. Zool. Lond.* 232 231-252.
- [28] Lees C, Vincent JEV and Hillerton JE 1991 Poisson's Ratio in Skin *Biomed. Mater. Eng.* 1 19-23.
- [29] Williams JL and Lewis JL 1982 Properties and an Anisotropic Model of Cancellous Bone from the Proximal Tibial Epiphysis *Trans. ASME, J. Biomech. Eng.* 104 50-56.
- [30] Liulan L, Qingxi H, Xianxu H and Gaochun X 2007 Design and Fabrication of Bone Tissue Engineering Scaffolds via Rapid Prototyping and CAD *Journal of Rare Earths* 25(2) 379-383.
- [31] Pan Y, Dong S, Hao Y, Chu T, Li C, Zhang Z and Zhou Y 2010 Demineralized Bone Matrix Gelatin as Scaffold for Tissue Engineering *African Journal of Microbiology Research* 4(9) 865-870.
- [32] Yang W, Li ZM, Shi W, Xie BH and Yang MB 2004, Review on Auxetic materials *Journal of Materials Science* 39 3269-79.
- [33] Gaspar N, Smith CW, Miller EA, Seidler GT and Evans KE 2005

Quantitative Analysis of the Microscale of Auxetic Foams. *Phys Status Solidi* 242(2)550-60.

- [34] Alderson A, Rasburn J, Evans KE and Grima JN 2001 Auxetic Polymeric Filters Display Enhanced De-Fouling and Pressure Compensation Properties *Membrane Technology* 137 6-8.
- [35] Grima JN, Jackson R, Anderson A and Evans KE 2000 Do Zeolites Have Negative Poisson's Ratios? *Adv. Materials* 12 1912-1918.
- [36] Grima JN, Alderson A and Evans KE 2005 Auxetic Behaviour from Rotating Rigid Units *phys. Stat. Sol. (b)* 242 561-575.